Structural and biochemical basis of apoptotic activation by Smac/DIABLO

Jijie Chai*, Chunying Du†, Jia-Wei Wu*, Saw Kyin*, Xiaodong Wang† & Yigong Shi*

* Department of Molecular Biology, Princeton University, Washington Road, Princeton, New Jersey 08544, USA
† Howard Hughes Medical Institute and Department of Biochemistry, University of Texas Southwestern Medical Center, Dallas, Texas 75235, USA

Apoptosis (programmed cell death), an essential process in the development and homeostasis of metazoans, is carried out by caspases. The mitochondrial protein Smac/DIABLO performs a critical function in apoptosis by eliminating the inhibitory effect of IAPs (inhibitor of apoptosis proteins) on caspases. Here we show that Smac/DIABLO promotes not only the proteolytic activation of procaspase-3 but also the enzymatic activity of mature caspase-3, both of which depend upon its ability to interact physically with IAPs. The crystal structure of Smac/DIABLO at 2.2 Å resolution reveals that it homodimerizes through an extensive hydrophobic interface. Missense mutations inactivating this dimeric interface significantly compromise the function of Smac/DIABLO. As in the *Drosophila* proteins Reaper, Grim and Hid, the amino-terminal amino acids of Smac/DIABLO are indispensable for its function, and a seven-residue peptide derived from the amino terminus promotes procaspase-3 activation *in vitro*. These results establish an evolutionarily conserved structural and biochemical basis for the activation of apoptosis by Smac/DIABLO.

Apoptosis is crucial in the development and homeostasis of all multicellular organisms[1–4]. Abnormal inhibition of apoptosis is a hallmark of cancer and autoimmune diseases, whereas excessive cell death is implicated in neurodegenerative disorders such as Alzheimer disease[5,6]. The mechanism of apoptosis is remarkably conserved across species, involving a cascade of initiator and effector caspases that are activated sequentially[7,8].

Caspases, a family of cysteine proteases with aspartate substrate specificity, are produced in cells as catalytically inactive zymogens[7]. Effector caspases, such as caspase-3, are activated by initiator caspases, such as caspase-9, through proteolytic cleavage at specific internal Asp residues[7]. Once activated, the effector caspases are responsible for proteolytic cleavage of a range of cellular targets, ultimately leading to cell death.

The inhibitor of apoptosis (IAP) family of proteins, originally identified in the genome of baculovirus on the basis of their ability to suppress apoptosis in infected host cells, has a key function in the negative regulation of programmed cell death in a variety of organisms[9,10]. IAPs suppress apoptosis by preventing the activation of procaspases and inhibiting the enzymatic activity of mature caspases[9,10]. Several distinct mammalian IAPs including XIAP, c-IAP1, c-IAP2 and survivin have been identified, and they all exhibit anti-apoptotic activity in cell culture[9,10]. In *Drosophila*, the anti-apoptotic activity of IAPs is removed by Reaper, Grim and Hid, all of which appear to act upstream of IAPs and interact physically with IAPs to relieve their inhibitory effect on caspase activation[11,12].

One important caspase activation cascade is triggered by the release of cytochrome *c* from the intermembrane space of mitochondria, which occurs in response to several apoptotic stimuli including serum deprivation, DNA damage and activation of cell-surface death receptors[13,14]. In the cytosol, cytochrome *c* associates with Apaf-1 in the presence of dATP or ATP and induces its oligomerization. The oligomeric Apaf-1 complex recognizes the inactive procaspase-9, forming the 'apoptosome', which induces autocatalytic processing of procaspase-9 (refs 15–19). The mature caspase-9 in turn activates its primary downstream target procaspase-3.

Concurrent with cytochrome *c* release, another important regulato of apoptosis, Smac[20] (second mitochondria-derived activator of caspases) or DIABLO[21], is also released from the mitochon-

Table 1 Summary of crystallographic analysis

	Resolution (Å)	Reflections: Measured	Reflections: Unique	Overall (outer shell): Data coverage (%)	Overall (outer shell): R_{sym} (%)	Heavy atom sites	MIR analysis (20–2.1 Å): All (outer shell) isomorphous difference (%)	MIR analysis (20–2.1 Å): Acentric/centric Phasing power	MIR analysis (20–2.1 Å): Acentric/centric Cullis R factor
Native 1	2.2	97,019	12,842	99.5 (97.8)	4.7 (24.2)				
EMP	2.9	23,398	4,671	80.7 (81.5)	9.9 (33.6)	5	23.7 (26.6)	1.65/1.28	0.67/0.65
HgAc	3.5	14,640	3,037	90.9 (92.4)	10.0 (30.2)	2	21.5 (23.7)	1.43/0.78	0.75/0.81
$K_2UO_2F_5$	3.6	9,213	2,830	88.0 (98.2)	10.2 (29.7)	4	29.8 (28.5)	1.11/0.71	0.85/0.82
$PhNH_2HgAc$	3.5	9,710	3,132	94.5 (95.0)	8.5 (23.8)	4	21.8 (25.7)	1.26/0.85	0.77/0.77
MeHgAc	3.5	7,738	2,826	87.7 (92.3)	10.2 (28.5)	4	19.5 (31.7)	0.90/0.53	0.85/0.89
Se-Met	3.4	20,598	6,057	96.9 (95.8)	10.2 (24.9)	4	16.0 (22.0)	1.12/0.76	0.82/0.78
Thimerosal	3.2	18,133	4,285	98.5 (99.0)	10.7 (33.2)	4	16.0 (30.4)	1.45/0.94	0.73/0.75

Mean figure of merit (20.0–3.0 Å): 0.588

Refinement	Resolution range	Reflections ($F > 2\sigma$)	Atoms modelled (total, water)	$R_{working}/R_{free}$ (%)	r.m.s. deviation: Bonds (Å)	r.m.s. deviation: Angles (deg)	r.m.s. deviation: B factor (Å²)
	15.0–2.2	11,728	1,420,47	24.5/25.9	0.005	1.0120	3.880

Se-Met: selono-methionine-derivatized Smac. $R_{sym} = \Sigma_h\Sigma_i|I_{hi} - I_h|/\Sigma_h\Sigma_i I_{hi}$, where I_h is the mean intensity of the i observations of symmetry related reflections of h. Isomorphous difference = $\Sigma||F_{PH}| - |F_P||/\Sigma|F_P|$, where F_P and F_{PH} are the native and derivative structure factor amplitudes, respectively. Phasing power = $[\Sigma F_{H(calc)}^2/\Sigma(F_{PH(obs)} - F_{PH(calc)})^2]^{1/2}$, where $F_{H(calc)}$ and $F_{PH(obs)}$ are the observed and calculated derivative structure factors, respectively. Cullis R factor = $\Sigma||F_{PH}| \pm |F_P| - F_{H(calc)}|/\Sigma|F_{PH} - F_P|$, where $F_{H(calc)}$ is the calculated heavy atom structure factor. Figure of merit = $|(\int P(\alpha)\exp(i\alpha)d\alpha)/\int P(\alpha)d\alpha|$, where $P(\alpha)$ is the probability distribution for the phase α. $R = \Sigma||F_{obs} - F_{calc}|/\Sigma F_{obs}$, where $F_{obs} = F_P$, and F_{calc} is the calculated protein structure factor from the atomic model (R_{free} was calculated with 5% of the reflections). r.m.s. in bond lengths and angles are the deviations from ideal values, and the r.m.s. deviation in B factors is calculated between bonded atoms.

articles

dria into the cytosol. Whereas cytochrome *c* induces multimerization of Apaf-1 to activate procaspase-9 and -3, Smac eliminates the inhibitory effect of many IAPs[20,21]. Smac interacts with all IAPs that have been examined, including XIAP, c-IAP1, c-IAP2 and survivin[20,21]. Thus, Smac appears to be a master regulator of apoptosis in mammals and a functional homologue of the *Drosophila* proteins Reaper, Grim and Hid.

Smac is synthesized as a 239-amino-acid precursor molecule; the amino-terminal 55 residues serve as the mitochondria targeting sequence, which is removed after import[20]. The mature form of Smac contains 184 amino acids and behaves as an oligomer in solution[20]. Despite its importance in cell death, no structural information is available on Smac or on its *Drosophila* functional homologues Reaper, Grim and Hid.

Here, we report the 2.2 Å resolution crystal structure of mature Smac, which shows an arch-shaped homodimer with rich surface features. The homodimeric interface is dominated by hydrophobic residues through van der Waals interactions. Mutations of key residues at the interface disrupt dimer formation and significantly weaken the ability of Smac to activate procaspase-3 and promote the enzymatic activity of mature caspase-3. In addition, the N-terminal residues of mature Smac are essential for Smac function, as mutation of the first amino acid renders the resulting protein completely inactive. Furthermore, we show that the N-terminal peptides of Smac can promote procaspase-3 activation *in vitro*, suggesting therapeutic potential. Combining structural, mutational and biochemical analyses, we propose a coherent model for apoptotic activation by Smac.

Structure of a Smac monomer

The mature form of Smac (residues 1–184; relative molecular mass 21,000 (M_r 21K)) was overexpressed in bacteria, purified to homogeneity and crystallized. The X-ray structure was determined at 2.2 Å resolution by multiple isomorphous replacement (Table 1). Our final atomic model contains residues 11–182. No electron density is seen corresponding to the N-terminal 10 residues, and we presume that this region is disordered in solution.

The Smac monomer is an elongated three-helix bundle with moderate curvature (Fig. 1a). The H1 helix packs closely against helices H2 and H3, whereas H2 and H3 are farther apart. Most of the hydrophobic residues are located in the interior of the three-helix bundle, contributing to its stability. In addition, the elongated helices are buttressed by 23 intra- and 9 interhelical hydrogen bonds involving the side chains of exposed polar residues. Owing to its elongated shape, Smac is expected to exhibit a much larger radius of hydration in solution than a globular protein with the same molecular mass.

Around half of the exposed hydrophobic residues cluster on one small surface patch formed by the N-terminal half of H1 and the carboxy-terminal third of H2 (Fig. 1a), indicating that this region might be involved in important protein–protein interactions.

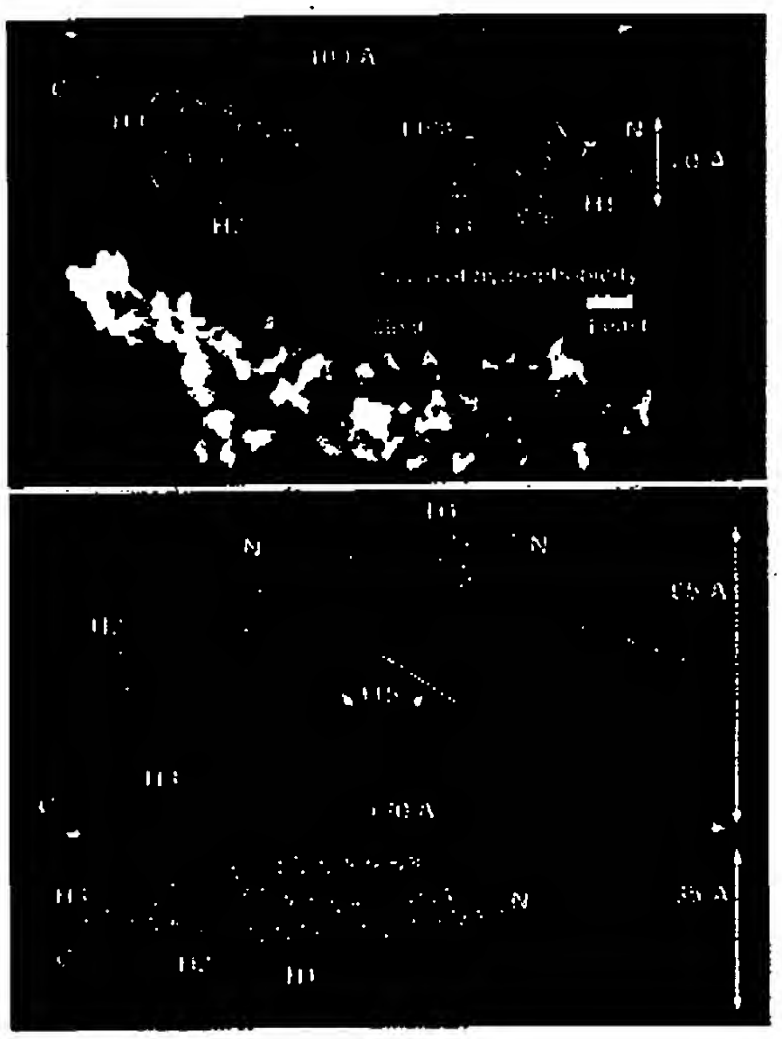

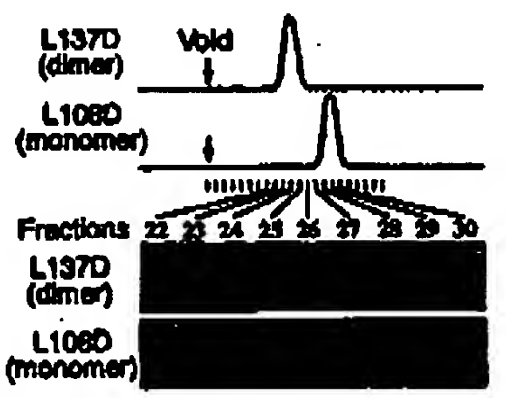

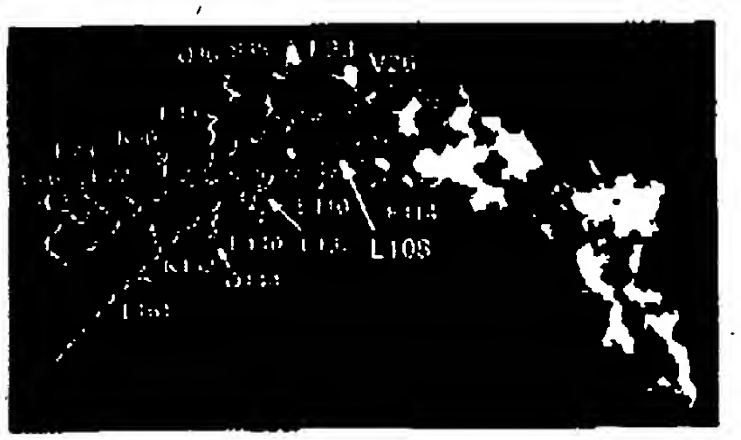

Figure 1 Schematic representation of Smac structure. **a**, The elongated structure of a Smac monomer. The hydrophobic surface patch is dark blue (bottom) and its constituent residues are yellow (top). **b**, The arch-shaped structure of a Smac dimer, with the two monomers coloured cyan and pink, respectively. The two views of the structure are related by a 90° rotation around a horizontal axis. Three critical residues at the dimeric interface, V26, F33 and L108, are coloured yellow and green for two Smac molecules. **c**, Representative chromatographs of Smac dimer (L137D) and monomer (L108D) mutants on gel filtration. We applied 0.5 mg of each of the 22 missense mutant proteins to gel-filtration chromatography, and the protein-containing fractions were visualized by SDS–polyacrylamide gel electrophoresis. **d**, Mapping of residues targeted for missense mutation on Smac structure. Mutation of the three red residues, V26, F33 and L108, completely disrupted Smac dimers, whereas mutation of all other residues (yellow) had no detectable effect. The two Smac monomers are shown in the same orientation as in **b** except one is represented by hydrophobic surface. Figs 1 and 2 were prepared using MOLSCRIPT[36] and GRASP[37].

Overall structure of a Smac dimer

Smac was reported to behave as an oligomer in solution, with an apparent M_r of 100K (ref. 20). Because Smac exhibits the same oligomeric state in both physiological buffer and crystallization solution, the oligomeric interface of Smac is probably preserved in crystal packing. We therefore carefully examined the crystal packing of one protomer against its neighbours. Unexpectedly, we failed to identify any protomer–protomer interface that can be propagated to form a higher-order oligomer, indicating that Smac may be a dimer in solution. Our analysis identified a strong candidate dimer interface.

In the crystals, two protomers of Smac pack symmetrically across the previously identified hydrophobic surface patch formed by helices H1 and H2, resulting in the burial of 2,157 Å^2 surface area (Fig. 1b). Dimerization through this interface creates a further elongated and arch-shaped Smac molecule, with the N termini on top and the carboxy termini at the feet of the arch (Fig. 1b). The angle subtended by the two legs of the arch is around 115°. There is an extensive flat surface underneath the arch formed by the C-terminal third of helix H2 and the N-terminal third of helix H3. The overall dimensions of the Smac dimer are length 130 Å, height 65 Å and width 35 Å, as measured by the corresponding backbone Cα atoms. This structural arrangement would cause a Smac dimer to exhibit a much greater apparent molecular mass in gel-filtration chromatography than the predicted theoretical weight.

To define the dimeric interface conclusively, we generated 22 missense mutations for specific surface residues in Smac, 15 of which targeted crystal packing contacts (Table 2). In particular, seven mutations were directed at residues at the observed dimeric interface (Table 2). All 22 mutant proteins were purified to homogeneity, and the oligomeric states of these proteins were individually analysed by gel-filtration chromatography (Fig. 1c, Table 2). Four point mutations (V26D, F33A, F33D and L108D), affecting three residues at the candidate dimeric interface, completely disrupted the oligomeric state of the wild-type protein (Fig. 1c, Table 2). The elution volume of these four mutants on gel filtration corresponds to an apparent M_r of about 33K, consistent with that expected for an elongated monomer (21K). In contrast, the other 18 mutations, including eight targeting other crystal packing contacts, had no detectable effect on the oligomeric state of Smac (Table 2). Because of the extensive and hydrophobic nature of the dimeric interface, mutation of a hydrophobic residue to alanine (V26A or L108A), or of a peripheral polar residue (Q36A), is not sufficient to abolish dimer formation (Fig. 1d, Table 2). These results confirm that Smac forms a symmetric dimer (Fig. 1b).

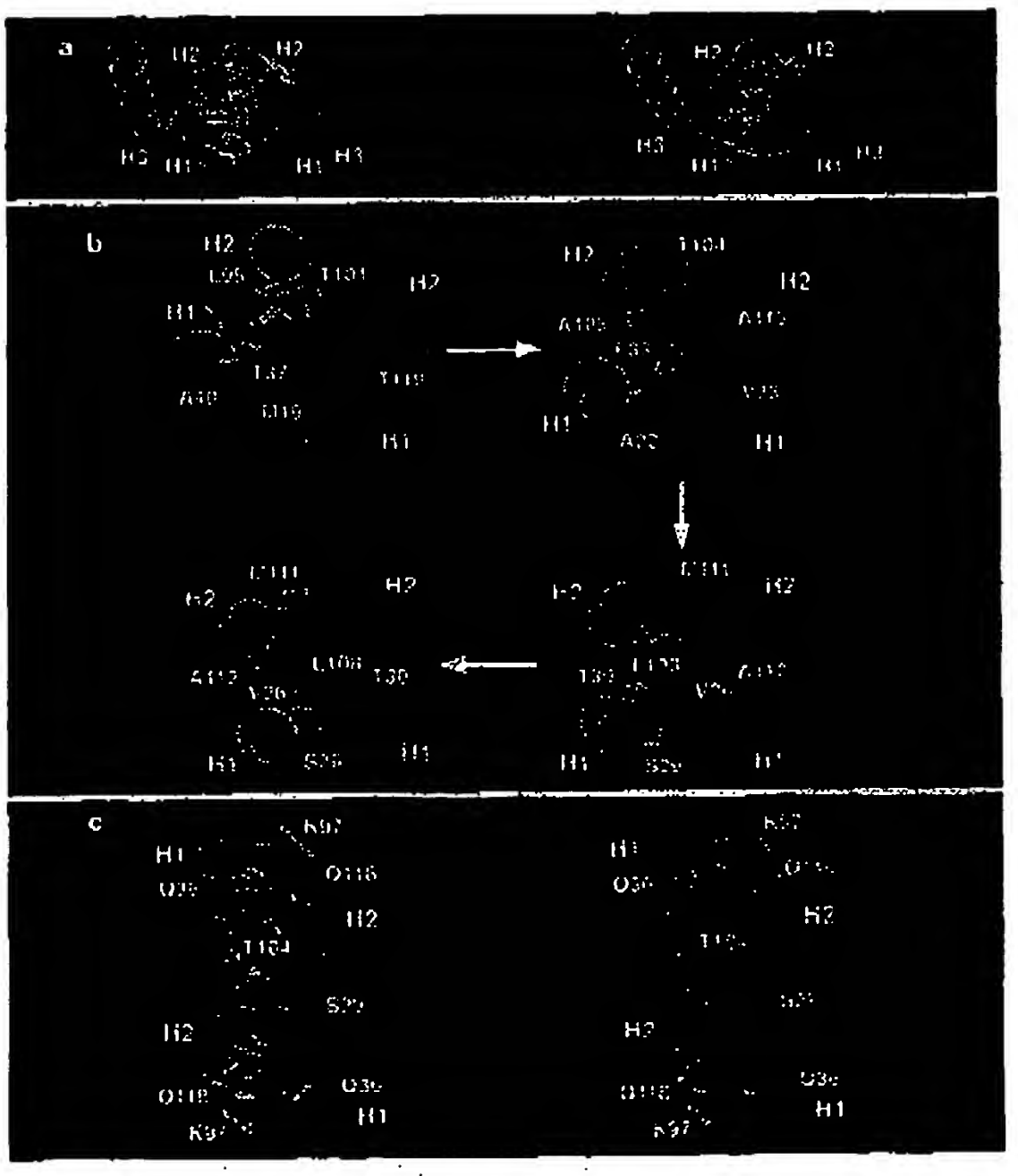

Figure 2 Specificity at the dimeric interface. a, Stereo diagram of the dimeric interface in Smac. The two Smac molecules are coloured cyan and pink. Interface residues from these two molecules are highlighted in yellow and green, respectively. Hydrogen bonds are represented by red dashed lines. b, Close-up views of the hydrophobic interactions at the interface. The four panels show four consecutive planes of interface packing from the outside to the centre of the four-helix bundle. The orientation of helices and the colour scheme are as in a. c, Stereo representation of the seven hydrogen bonds, represented by red dashed lines, at the dimeric interface.

Specificity at the dimeric interface

Two molecules of Smac homodimerize through their N-terminal thirds of helix H1 and C-terminal thirds of helix H2, forming an antiparallel four-helix bundle (Fig. 2a). The core interface is predominantly hydrophobic, with additional specificity provided by intermolecular hydrogen bonds at the periphery of the four-helix bundle (Fig. 2).

The hydrophobic packing at the dimeric interface is extensive, with 18 residues from one molecule interacting with those from the other molecule (Fig. 2a, b). The interface exhibits twofold symmetry, with each half consisting of three planes of interdigitating residues (Fig. 2b). Hydrophobic residues stack closely against each other both within and between adjacent planes. At the end of the four-helix bundle lies the first plane, where two Thr residues, T37 and T101, on molecule 1, pack against M19 and T119 on molecule 2 (Fig. 2b). Farther along the axis of the four-helix bundle is the second plane, where F33 on H1 extends into the centre (Fig. 2b). Five small residues, A105 and T104 on molecule 1 and A22, V23 and A115 on molecule 2, form a hydrophobic environment around F33. The third plane is located next to the centre of the four-helix bundle (Fig. 2b). Within this plane, L108 on molecule 1 and V26 on molecule 2 pack closely against each other at the centre. Four additional residues, T30 and S29 on helix H1 of molecule 1 and M111 and A112 on helix H2 of molecule 2, pack at the periphery of this plane, forming a network of van der Waals interactions.

Three residues, V26, F33 and L108, reside in the centre of the four-helix bundle and constitute the core of the hydrophobic interface (Fig. 2b). This structural arrangement predicts that replacement of these residues by charged residues is thermodynamically unfavourable and probably destabilizes the dimeric interface. Indeed, V26D, F33D and L108D all led to complete disruption of the dimeric interface (Fig. 1c, Table 2). Replacement of the bulky F33 by a small Ala residue also abrogated dimer formation (Table 2).

Although hydrophobic contacts are important in the formation of a Smac dimer, hydrogen-bond interactions may further strengthen the interface and probably contribute to the specificity. There are seven intermolecular hydrogen bonds at the interface, all located at the periphery (Fig. 2c). At the end of the four-helix bundle, the side chain of K97 donates a hydrogen bond to the backbone carbonyl oxygen of Q118, whereas its side chain accepts a hydrogen bond from T104 (Fig. 2c). The side chain of Q36 makes a hydrogen bond to the backbone carbonyl group of L18 (Fig. 2c). At the centre of the helix bundle, S29 makes a symmetric contact to S29 in the other molecule (Fig. 2c).

Interaction with IAPs

Smac stimulates activation of procaspase-3 by relieving inhibition by IAPs[20,21]. All members of the IAP family contain at least one BIR (baculoviral IAP repeat) motif, and many contain three[9]. Recent experiments indicate that different BIR domains may exhibit distinct functions. During Fas-induced apoptosis, the endogenous XIAP is cleaved into two fragments, each with distinct specificity for caspases[22]. In addition, the second BIR domain (BIR2) of XIAP appears to be a potent suppressor of apoptosis and a direct inhibitor for caspases, whereas neither BIR1 nor BIR3 exhibit similar activity[23].

To characterize Smac–IAP interaction further, we generated a series of XIAP fragments as fusion proteins with glutathione *S*-transferase (GST; Fig. 3a) and assayed their interaction with Smac using purified recombinant proteins (Table 2). As expected, wild-type Smac interacts stably with the second or third BIR domain of XIAP (Table 2). In contrast, Smac exhibited no detectable interaction with XIAP-BIR1 despite its strong sequence homology to the other two BIR domains (Table 2). To examine whether Smac can

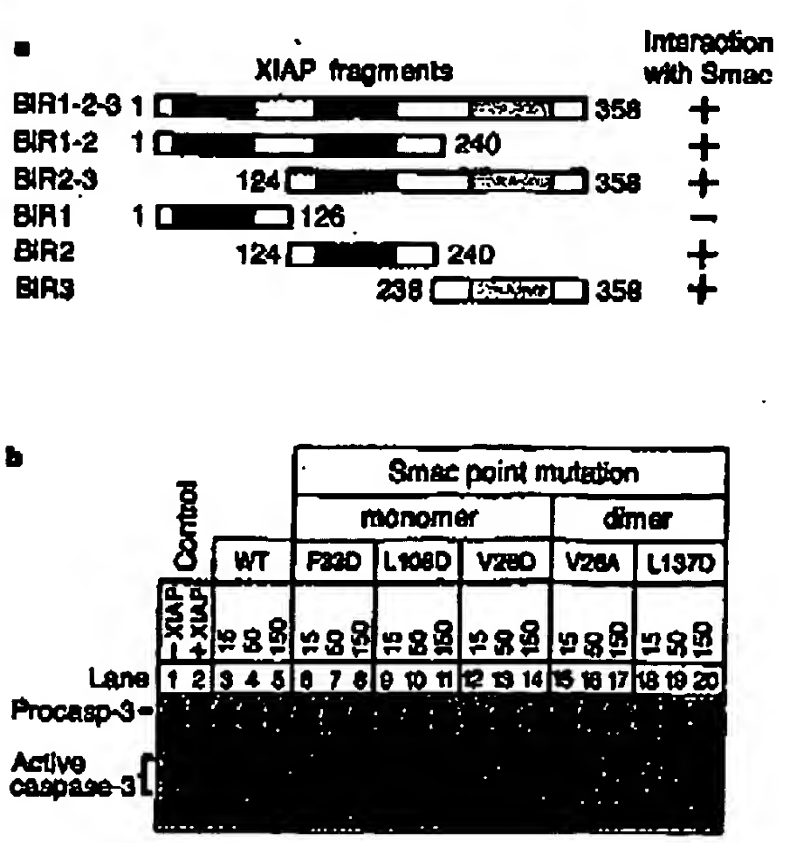

Figure 3 Functional significance of the dimeric interface in Smac. **a**, Schematic diagram of the XIAP fragments and results of their interaction with Smac. All fragments were expressed and purified as GST-fusion proteins. **b**, Missense mutations inactivating dimer formation exhibited severely diminished activation of procaspase-3. Lane 1, positive control in which procaspase-3 was converted to active caspase-3 in a totally reconstituted system containing purified recombinant Apaf-1, procaspase-9, cytochrome *c* and dATP. Lane 2, inhibition of procaspase-3 activation by XIAP. The same amount of XIAP was used for all other lanes. Numbers indicate Smac concentrations (nM). **c**, Smac missense mutations that inactivate dimer formation fail to release XIAP inhibition of caspase-3 activity. The amounts of wild-type Smac were 3, 0.1, 0.3, 1, 3 and 3 μg for lanes 3, 6, 7, 8, 9 and 10, respectively. We used 3 μg of each of the mutant proteins for lanes 11–13. **d**, Missense mutations inactivating dimer formation disrupted interaction with the BIR2 domain of XIAP. The interaction was examined by GST-mediated pull-down assays. For each Smac mutant, the left and right lanes indicate the input protein and the final complex, respectively.

bind simultaneously to BIR2 and BIR3 of XIAP, we performed competition experiments. The results show that BIR2 and BIR3 exclude each other upon binding to Smac (data not shown).

In contrast to the wild-type dimeric Smac, the monomeric mutants V26D, F33D and L108D could not interact with the BIR2 domain of XIAP (Table 2). A fourth monomeric mutant, F33A, had severely diminished binding activity for XIAP-BIR2 (Table 2). All dimeric Smac mutants retained their ability to interact with XIAP-BIR2 (Table 2). Surprisingly, both monomeric and dimeric missense mutants can interact with XIAP-BIR3 (Table 2). In addition to its significance for the mechanism of caspase activation, this result also implies distinct specificity in the function of different BIR domains.

Dual effects of Smac

Smac can induce activation of procaspase-3 by eliminating the inhibitory effect of IAPs[20]. To characterize this function *in vitro*, we reconstituted a procaspase-3 activation assay, using purified recombinant components (Fig. 3b). In the presence of Apaf-1, procaspase-9, cytochrome *c* and dATP, the radio-labelled procaspase-3 precursor was converted to the active form consisting of two subunits (Fig. 3b, lane 1). Addition of the recombinant XIAP protein (residues 1–356) completely inhibited the proteolytic processing of procaspase-3 (lane 2). The inhibitory effect of XIAP was eliminated by increasing amounts of wild-type Smac (lanes 3–5).

Apoptosis is carried out by the enzymatic activity of mature caspases. Although Smac induces the activation of procaspase-3, it is not clear whether it can also promote the catalytic activity of mature caspases. To investigate this possibility, we used a caspase-3 enzymatic assay, in which caspase-3 activity is monitored through its cleavage of DFF45 (ref. 24) or ICAD[25], the inhibitory subunit of the caspase-activated DNase. In apoptotic cells, degradation of DFF45 or ICAD releases inhibition of the DNase DFF40 or CAD, which subsequently cleaves chromosomes into nucleosomes[25,26]. In the absence of caspase-3, the DFF complex remains inactive and the DNA substrate remains intact (Fig. 3c, lane 1). Incubation with active caspase-3 releases the DNase activity of DFF40, which degrades the DNA substrate into short oligonucleotides (Fig. 3c, lane 4). Here the enzymatic activity of caspase-3 is measured as its ability to activate DFF40/45, which in turn cleaves DNA. Addition of XIAP-BIR2 to this reaction completely inhibits the enzymatic activity of caspase-3, as indicated by the absence of DNA cleavage (Fig. 3c, lane 5). Neither BIR1 nor BIR3 has any effect (data not shown), presumably because neither can bind caspase-3 (ref. 23). With the addition of increasing amounts of wild-type Smac, the inhibitory effect of XIAP on caspase-3 was relieved and the DNA was cleaved into progressively lower molecular mass species (Fig. 3c, lanes 6–9).

These observations show that Smac promotes the enzymatic activity of caspase-3 by physically removing the inhibitory effect of IAPs. Our results demonstrate that Smac has two roles: to induce the activation of procaspase-3, and to promote the enzymatic activity of mature caspase-3.

Functional significance of a Smac dimer

We first examined the role of the Smac dimer in the induction of procaspase-3 activation using the *in vitro* reconstituted assay (Fig. 3b). In contrast to wild-type Smac (Fig. 3b, lanes 3–5), the three monomeric Smac mutants, V26D, F33D and L108D, had markedly less capacity to promote procaspase-3 activation (Fig. 3b, lanes 6–14). Two dimeric Smac mutants, V26A and L137D, retained similar activity to wild-type Smac (Fig. 3b, lanes 15–20). These results indicate that Smac dimerization is essential to its function in activating procaspase-3.

Next we investigated the significance of a Smac dimer in promoting the enzymatic activity of mature caspase-3 (Fig. 3c). In contrast to wild-type Smac (Fig. 3c, lanes 6–9), the monomeric Smac mutants could not relieve the inhibition of caspase-3 activity by XIAP (Fig. 3c, lanes 11, 12). The activity of the dimeric mutant V26A was similar to that of the wild-type Smac (Fig. 3c, lane 13). Thus Smac promotes the enzymatic activity of caspase-3, and Smac dimerization is essential to this activity.

The functional dependence on dimerization of Smac can be explained by existing evidence and our interaction data (Fig. 3d).

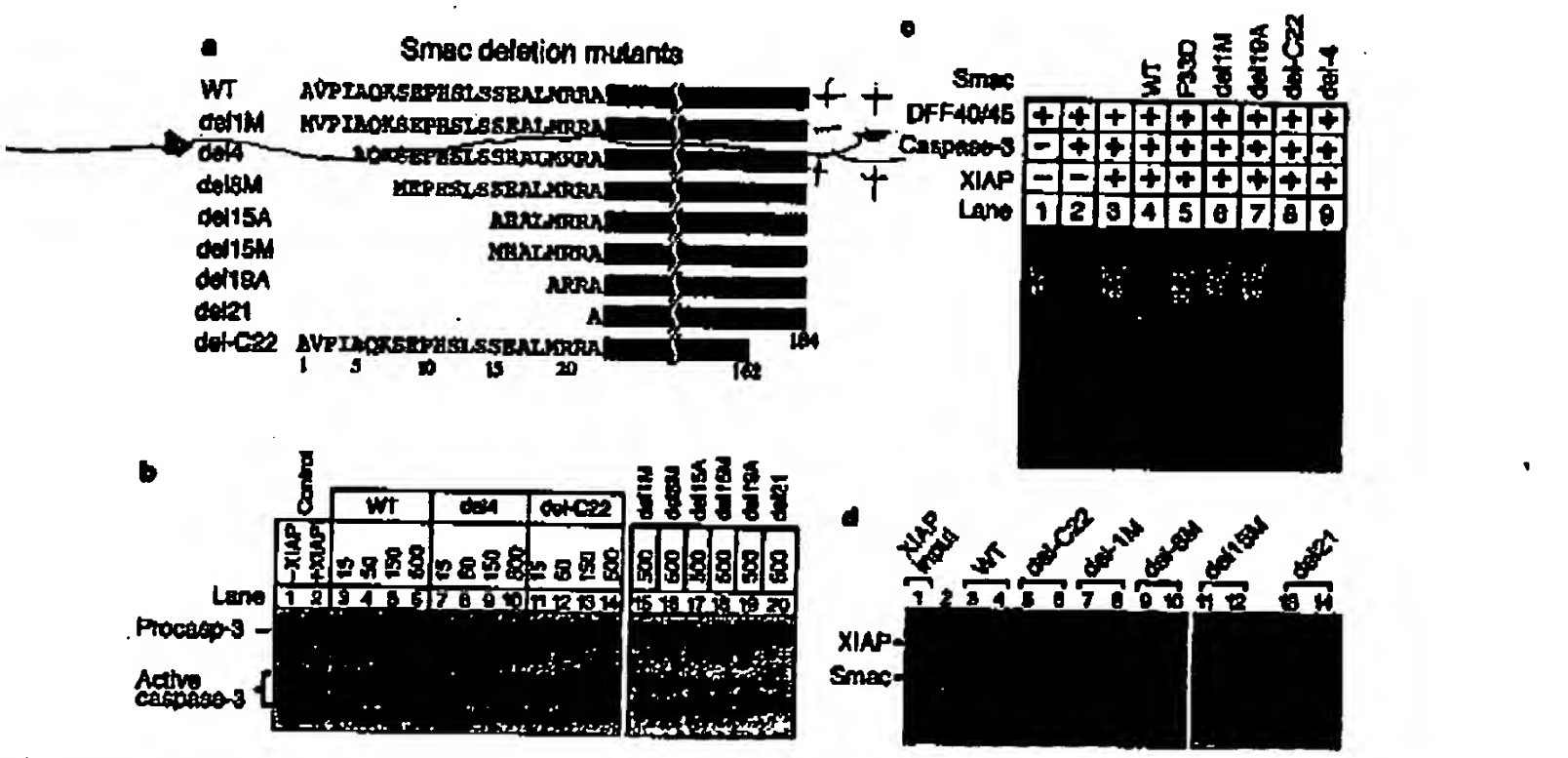

Figure 4 Functional significance of the N terminus of Smac. a, Smac N-terminal deletion mutants. The indicated sequences of N termini were confirmed by peptide sequencing. b, N-terminal deletion mutants exhibited severely diminished activation of procaspase-3. The concentrations of wild-type and mutant Smac are indicated in nM. c, N-terminal deletion mutants failed to remove the inhibition of caspase-3 activity by XIAP. The amount of wild-type or mutant Smac protein used was 3 μg (lanes 4–9). d, N-terminal deletion mutants cannot interact with the XIAP BIR2. The interaction was examined using GST-mediated pull-down assays. For each Smac mutant, the left and right lanes indicate the input protein and the final complex, respectively.

The second BIR domain of XIAP is uniquely potent in blocking the ...tion of procaspase-9 and in inhibiting the enzymatic activity ...ture caspase-3 (ref. 23). However, monomeric Smac mutants failed to interact with XIAP-BIR2 (Fig. 3d, Table 2), thus making these mutants unable to induce procaspase-3 activation and promote the enzymatic activity of mature caspase-3 by relieving the inhibitory effect of XIAP.

Function of N-terminal residues in Smac

In the course of preparing recombinant proteins for biochemical assays, we discovered that Smac protein derived from an N-terminal GST fusion is completely inactive even after removal of GST by proteolysis. This result indicates that the N-terminal flexible sequences in Smac may be critical for its activity.

To investigate systematically the role of the N-terminal sequences, we generated a series of Smac mutants with N-terminal deletions (Fig. 4a). All mutant proteins were purified to homogeneity. The identities of these mutants were confirmed by mass spectroscopic analysis and N-terminal peptide sequencing. The first residue in endogenous wild-type Smac is Ala, owing to cleavage of the mitochondria targeting sequence[28]. The initiation Met residue is completely removed in bacterial expression owing to the presence of an Ala as the penultimate residue[27] (Fig. 4a). We attempted to create a single-residue deletion by removing this Ala. However, the initiation Met is no longer removed owing to the presence of a Val as the penultimate residue[27]. In essence, a single point mutation (Ala to Met) was created instead and this mutant was named del1M. The rest of the mutants were similarly created and named (Fig. 4a).

We assayed these N-terminal deletion mutants for their ability to promote caspase-3 activation (Fig. 4b). The missense mutation at the first residue, del1M, completely eliminated Smac activity (...4b, lane 15). All other deletion mutants, with the exception ...4, also lost their ability to promote procaspase-3 activation (Fig. 4b, lanes 16–20). Interestingly, the mutant in which the N-terminal four residues were removed (del4) was partially active (Fig. 4b, lanes 7–10). This mutation resulted in clean removal of the first four residues and thus partially preserved the identity of the N-terminal sequence (Fig. 4a). Removal of the C-terminal 22 residues in Smac (del-C22) had no impact on its ability to promote caspase-3 activation (Fig. 4b, lanes 11–14).

We assayed these N-terminal deletion mutants for their ability to promote the enzymatic activity of caspase-3 (Fig. 4c). Wild-type Smac relieved the inhibitory effect of XIAP (Fig. 4c, lanes 4), but the Smac N-terminal deletion mutants were completely inactive in this assay (Fig. 4c, lanes 6, 7). In contrast, the activity of the C-terminal deletion mutant (del-C22) was indistinguishable from that of wild-type Smac (Fig. 4c, lane 8); del4 was also partially active (Fig. 4c, lane 9).

These results show that the N-terminal sequences are required for Smac function. None of the deletions affects the dimeric interface and all deletion mutants examined behave as homodimers in solution (Table 2), ruling out the possibility that the loss of function for these deletions was due to disruption of the dimeric interface. Because Smac works by interacting with IAPs, we hypothesized that these N-terminal deletions may have removed its ability to interact with IAPs. None of the loss-of-function deletion mutants could interact with XIAP (Fig. 4d, Table 2). Consistent with its weak activity, the mutant del4 retained weak interaction with XIAP (Table 2).

N-terminal peptides activate procaspase-3

To examine whether the N-terminal peptides themselves might be able to promote activation of procaspase-3, several Smac peptides were chemically synthesized, purified, and assayed for their function (Fig. 5). The assay was identical to that shown in Fig. 3b, with the same set of control experiments (Fig. 5b, lanes 1–6). For comparison, we also included the result for a Smac monomer mutant (Fig. 5b, lanes 7–9). A peptide consisting of the first seven residues of Smac, Smac-7, could promote procaspase-3 activation at around 10 μM, and this activity reached its maximum at 300 μM (Fig. 5b, lanes 11–14). The same result was obtained for Smac-10 (Fig. 5b, lanes 16–19), Smac-11 and Smac-16 (data not shown). In contrast, Smac-7M, which differs from Smac-7 only in its first residue (Fig. 5a), had no detectable activity at 300 μM (Fig. 5b, lane 15). Another negative control peptide, Smac-7R, which corresponds to the reversed version of Smac-7, was also inactive for procaspase-3 activation (Fig. 5b, lane 10).

Table 2 Properties of Smac mutants

Smac mutant	Oligomeric state	Interaction with XIAP: BIR1 (1–125)	BIR2 (124–240)	BIR3 (238–368)	BIR1-2-3 (1–355)
WT	dimer	No	Yes	Yes	Yes
V26D*	monomer	No	No	Yes	Yes
V26A*	dimer	No	Yes	Yes	Yes
F33D*	monomer	No	No	Yes	Yes
F33A*	monomer	No	weak	Yes	Yes
Q39A*	dimer	No	Yes	Yes	Yes
L109D*	monomer	No	No	Yes	Yes
L109A*	dimer	No	Yes	Yes	Yes
S38A†	dimer	No	Yes	Yes	Yes
E43A†	dimer	No	Yes	Yes	Yes
L137D†	dimer	No	Yes	Yes	Yes
L137A†	dimer	No	Yes	Yes	Yes
L140D†	dimer	No	Yes	Yes	Yes
L140A†	dimer	No	Yes	Yes	Yes
Q144A†	dimer	No	Yes	Yes	Yes
L161A†	dimer	No	Yes	Yes	Yes
del1M	dimer	No	No	No	No
del4	dimer	No	weak	weak	weak
del9M	dimer	No	No	No	No
del15A	N/A	No	No	No	No
del15M	N/A	No	No	No	No
del19A	N/A	No	No	No	No
del21	N/A	No	No	No	No
...22	dimer	No	Yes	Yes	Yes

* missense mutations target residues in the described dimeric interface (see text).
† these missense mutations target residues involved in other crystal packing contacts.
The following seven missense mutations targeting surface residues in Smac do not affect dimer formation: K50E, E72R, E73K, E76R, E110R, E110K and K152E.

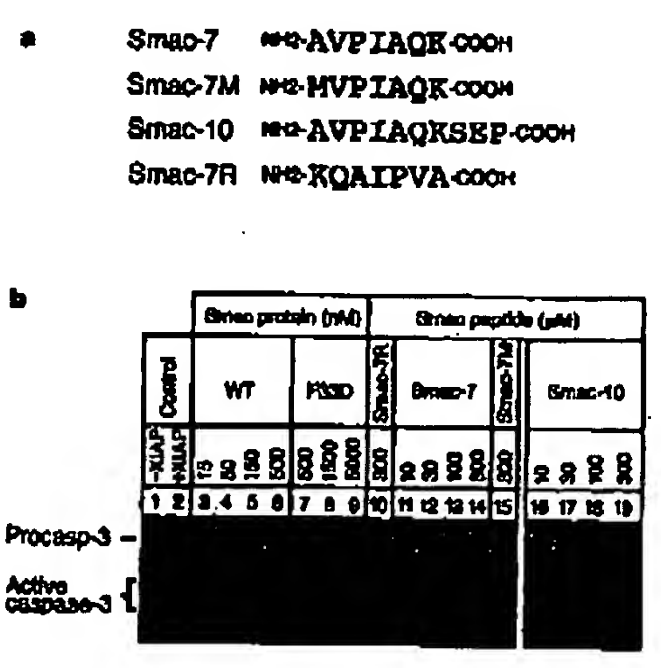

Figure 5 N-terminal peptides of Smac directly promote the activation of procaspase-3. a, The peptide sequences used in the assay. Smac-7 contains the N-terminal seven residues of Smac whereas Smac-7R represents the reversal of the sequence. b, Results of procaspase-3 activation assays. For comparison, the results of wild-type Smac protein and the F33D mutant are also shown (lanes 3–9).

Discussion

Despite high sequence similarity among the three BIR domains of XIAP, Smac interacts only with BIR2 and BIR3, not BIR1, indicating that the different BIR domains may have distinct functions. In addition, BIR2 and BIR3 exclude each other upon binding to Smac, indicating that they may recognize the same structural motif on Smac. N-terminal deletion mutants of Smac could not interact with either BIR domain (Table 2). Interestingly, the integrity of the dimeric interface is indispensable for interaction with BIR2 but not BIR3, indicating that the BIR2 domain might form a dimer in solution. In agreement with this proposal, BIR2 but not BIR3 can inhibit the catalytic activity of mature caspase-3 (ref. 23), which is a homodimer by itself[29]. Further supporting this hypothesis, the BIR motifs of the IAP protein Op-IAP mediate self-oligomerization[29]. Nevertheless, XIAP-BIR2 appeared to be a monomer in solution[30].

Interaction with IAPs depends on the integrity of the N terminus of Smac. This interaction appears to be highly specific, because any modification of the N-terminal residues in Smac compromised or abolished interaction. To our surprise, the replacement of the N-terminal residue Ala by Met in Smac completely abrogated interaction with IAPs, indicating that the N-terminal hydrophobic residues in Smac may fit tightly into a surface groove on the BIR domain (Fig. 6a). In this case, the mutation of a small Ala residue by a bulky Met could abrogate binding through steric hindrance. This hypothesis is consistent with the observation that the Smac mutant del4, which lacks the first four residues, retains binding (Table 2). All binding studies between Smac and XIAP have been reproduced using c-IAP1 fragments with identical results (data not shown). Thus it is likely that Smac interacts with XIAP, c-IAP1 and c-IAP2 in a similar manner (Fig. 6a).

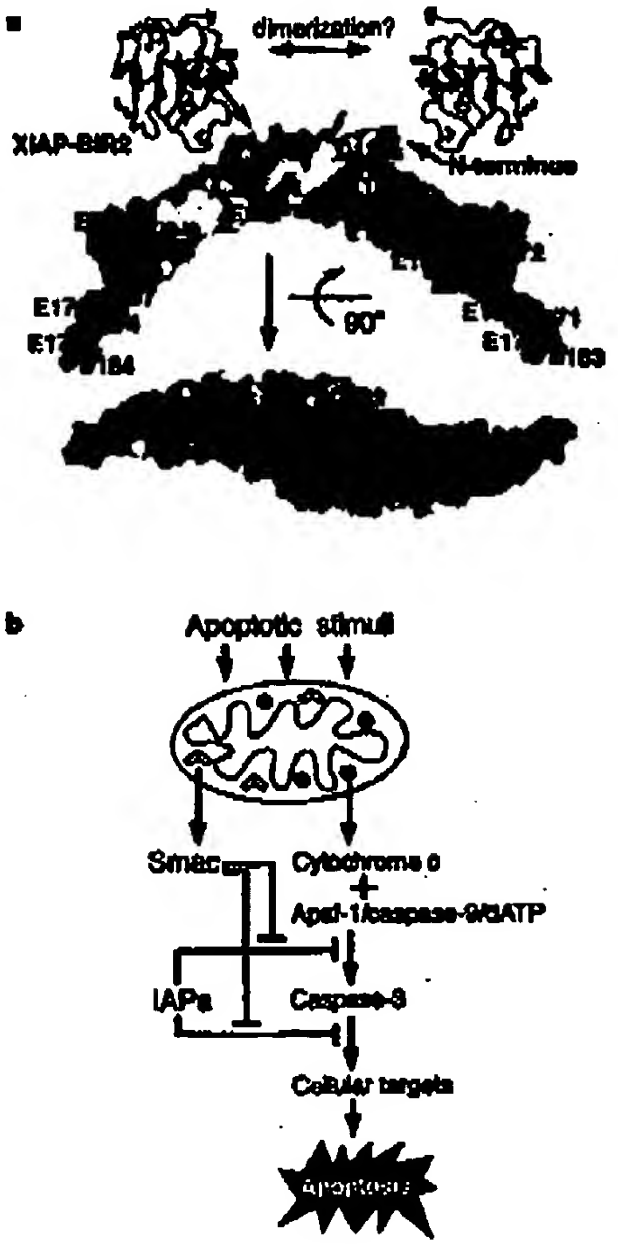

Figure 6 Model of Smac function. a, Model of interaction between Smac and IAPs. The surface of the Smac molecule is coloured by electrostatic potential, with negative and positive charges in red and blue, respectively. The BIR domain of IAPs, represented by XIAP-BIR2[30], is proposed to bind mainly the N-terminal sequences in Smac with additional contacts in the adjacent area. b, Model of Smac function. Smac not only induces the proteolytic activation of procaspase-3 but also promotes the catalytic activity of active caspase-3, both of which depend on its ability to bind IAPs.

Although indispensable, the N-terminal sequences of Smac do not appear to be sufficient for stable interaction with IAPs. First, Smac monomeric mutants, such as F33D and V26D, maintain an intact N terminus but do not bind BIR2. Because the N terminus of one Smac protomer lies near the other protomer, the additional binding sites probably include regions of this other molecule (Fig. 6a). Second, although the Smac peptides were functional, they achieved a similar level of caspase-3 activation at higher concentrations compared with the Smac monomeric mutants (Fig. 5).

Previous studies indicated that Smac can promote the activation of procaspase-3 by eliminating the inhibitory effect of IAPs[20]. We have shown that Smac promotes apoptosis through at least two mechanisms: inducing the proteolytic activation of procaspase-3 and promoting the enzymatic activity of mature caspase-3 (Fig. 6b). Both functions depend on the ability of Smac to interact physically with IAPs.

Smac functions as a dimer. Monomeric Smac exhibited 3–5-fold lower activation of procaspase-3 (Fig. 3b) but was largely inactive in promoting the enzymatic activity of mature caspase-3 (Fig. 3c). This is probably because monomeric Smac abrogated the interaction with the XIAP-BIR2 domain that is dominant in inhibiting caspase-3 activity[23]. As expected, the Smac peptides can promote the activation of procaspase-3 only at concentrations higher than the monomeric mutants (Fig. 5b).

The *Drosophila* IAP protein, DIAP1, suppresses apoptosis by inhibiting caspases. Three *Drosophila* proteins, Reaper, Grim and Hid, induce apoptosis by eliminating this inhibitory effect through physical interactions[11,12]. Thus Smac appears to be the mammalian functional homologue of Reaper, Grim and Hid. We have provided further evidence that the mechanisms by which Smac and Reaper/Grim/Hid activate apoptosis are conserved. Both Smac and Reaper/Grim/Hid contain an N-terminal fragment that is important for their function and for interactions with IAPs. The sequence homology among Reaper, Grim and Hid is restricted to their N-terminal 14 amino acids; deletion of these residues leads to loss of interaction with IAPs[9]. In addition, an N-terminal 37-residue peptide of Hid was sufficient to induce apoptosis and inhibit caspases in insect cells[11].

We also identified a 7-amino-acid peptide that can activate procaspase-3 activation. The high concentrations of this peptide required may be related to the amount of recombinant XIAP used in this experiment. Although untested, it is possible that even shorter peptides could possess similar activities. Thus, these peptides could be modified to test their ability to induce apoptosis in cancer cells that overexpress IAPs. □

Methods

Site-directed mutagenesis and protein preparation

We generated point mutations using a standard PCR-based cloning strategy, and verified the identities of individual clones through double-stranded plasmid sequencing. Both wild-type and mutant Smac were overexpressed in *Escherichia coli* strain BL21(DE3) as C-terminally 9-histidine-tagged proteins using a pET-15b vector (Novagen). Selenomethionyl Smac was expressed in *E. coli* B834(DE3) (Novagen) in M9 minimal medium supplemented with 50 mg l^{-1} selenomethionine. The soluble fraction of the fusion protein in the *E. coli* lysate was purified over a Ni-NTA (Qiagen) column, and further fractionated by anion-exchange (Source-15Q, Pharmacia) and gel-filtration chromatography (Superdex-200, Pharmacia). Recombinant XIAP and c-IAP1 fragments were overexpressed as GST-fusion proteins using pGEX-2T (Pharmacia). GST–IAP in the *E. coli* lysate was

purified over a glutathione sepharose column, and further purified by anion-exchange chromatography (Source-15Q).

F40/45 complexes were co-expressed in *Escherichia coli* strain BL21(DE3) and purified to homogeneity through anion-exchange (SP-sepharose and Source-15S) and gel-filtration chromatography (Superdex-200). Active caspase-3 was expressed as a C-terminally 6-histidine-tagged protein using a pET-21b vector (Novagen) and purified as described above.

In vitro interaction assay

Interactions between Smac and IAPs were examined by GST-mediated pull-down assays. About 0.4 mg of a recombinant IAP fragment was bound to 200 µl of glutathione resin as a GST-fusion protein and incubated with 0.5 mg of wild-type or mutant Smac at room temperature. After extensive washing with an assay buffer containing 25 mM Tris, pH 8.0, 150 mM NaCl and 2 mM dithiothreitol (DTT), the complex was eluted with 5 mM reduced glutathione and visualized by SDS–PAGE with Coomassie staining.

Assay for activation of procaspase-3

Procaspase-3 was translated and purified as described[34]. An aliquot of the *in vitro* translated procaspase-3 (1 µl) was incubated with relevant proteins in the presence of 10 µM dATP at 30 °C for 1 h in a final volume of 20 µl in buffer A (20 mM HEPES-KOH, pH 7.5, 10 mM KCl, 2.5 mM $MgCl_2$, 1 mM DTT and 0.1 mM PMSF). Each reaction contained 38 nM recombinant Apaf-1, 12 nM recombinant procaspase-9 and 500 nM purified horse heart cytochrome *c*. The mouse XIAP fragment (residues 1–356) was used at 40 nM concentration to inhibit the reaction. At the end of incubation, 7 µl of 4×SDS sample buffer was added to each reaction, which was analysed by SDS–PAGE and phosphorimaging. The XIAP fragment used in this assay is derived from mouse, XIAP fragments used for all other assays are of human origin.

Assay for enzymatic activity of mature caspase-3

The reaction was carried out at 37 °C for 20 min in a final volume of 20 µl in a buffer containing 25 mM Tris, pH 8.0, 150 mM NaCl, 5 mM $MgCl_2$ and 100 µg ml^{-1} BSA. We used 0.25 µg of ICAD/CAD complex, 0.1 µg of active caspase-3 and 1 µg of GST–XIAP-BIR2 (residues 124–240) where indicated. In each reaction, 2 µg of pEMBL plasmid was used as a substrate for the activated CAD. The reactions were subjected to 2% agarose gel electrophoresis and stained with ethidium bromide.

Crystallization and data collection

Crystals were grown at 4 °C by the hanging-drop vapour-diffusion method by mixing protein (15 mg ml^{-1}) with an equal volume of reservoir solution containing 20% 1,4-dioxane (v/v), 200 mM ammonium sulphate and 10 mM DTT. The crystals grew over 3–4 weeks. The crystals are in the primitive hexagonal space group $P6_122$, with unit cell dimensions $a = b = 103.51$ Å, $c = 70.38$ Å, and contain one Smac molecule in each asymmetric unit. Diffraction data were collected using an R-AXIS-IV imaging plate detector mounted on a Rigaku 200HB generator. Derivatives were obtained by soaking crystals in appropriate heavy atom solutions under the condition of a cryoprotectant buffer containing 20% 1,4-dioxane (v/v), 200 mM ammonium sulphate and 20% glycerol (v/v). The concentration and soaking time for EMP, HgAc, $K_3UO_2F_5$, $PhNH_2HgAc$, MeHgAc and HgThimerosal were 0.5 mM/18 h, 0.5 mM/12 h, 1 mM/20 h, 2 mM/35 h, 2 mM/24 h and 0.5 mM/10 h, respectively.

Structure determination

The heavy atom positions of the EMP, HgAc and selenium derivative were determined using SOLVE[32] and further refined using MLPHARE[33]. The heavy atom sites of all other derivatives were identified using the difference Fourier method. Initial MIR phases calculated with the program MLPHARE[33] had a mean figure of merit of 0.586 to 3.0 Å resolution, and were improved with solvent flattening and histogram matching using program DM[35]. A model was built into MIR electron density maps with program O[36] and refined by simulated annealing using CNS[37]. The final refined atomic model contains Smac residues 11–182 and 47 water molecules. The N-terminal ten residues and the C-terminal two residues in Smac have no electron density in the maps, and we presume that these regions are disordered in the crystals.

Received 4 July; accepted 25 July 2000.

1. Steller, H. Mechanisms and genes of cellular suicide. *Science* 267, 1445–1449 (1995).
2. Jacobson, M. D., Weil, M. & Raff, M. C. Programmed cell death in animal development. *Cell* 88, 347–354 (1997).
3. Hengartner, M. O. Programmed cell death in invertebrates. *Curr. Opin. Genet. Dev.* 6, 34–38 (1996).
4. Horvitz, H. R. Genetic control of programmed cell death in the nematode *Caenorhabditis elegans*. *Cancer Res.* 59, 1701–1706 (1999).
5. Thompson, C. B. Apoptosis in the pathogenesis and treatment of disease. *Science* 267, 1456–1462 (1995).
6. Green, D. R. & Martin, S. J. The killer and the executioners how apoptotic controls malignancy. *Curr. Opin. Immunol.* 7, 694–703 (1995).
7. Thornberry, N. A. & Lazebnik, Y. Caspases: Enemies within. *Science* 281, 1312–1316 (1998).
8. Chinnaiyan, A. M. & Dixit, V. M. The cell-death machine. *Curr. Biol.* 6, 555–562 (1996).
9. Deveraux, Q. L. & Reed, J. C. IAP family proteins—suppressors of apoptosis. *Genes Dev.* 13, 239–252 (1999).
10. Miller, L. K. An exegesis of IAPs: salvation and surprises from BIR motifs. *Trends Cell Biol.* 9, 323–328 (1999).
11. Wang, S., Hawkins, C., Yoo, S., Müller, H.-A. & Hay, B. The *Drosophila* caspase inhibitor DIAP1 is essential for cell survival and is negatively regulated by HID. *Cell* 98, 453–463 (1999).
12. Goyal, L., McCall, K., Agapite, J., Hartwieg, E. & Steller, H. Induction of apoptosis by *Drosophila* reaper, hid and grim through inhibition of IAP function. *EMBO J.* 19, 589–597 (2000).
13. Zou, H., Henzel, W. J., Liu, X., Lutschg, A. & Wang, X. Apaf-1, a human protein homologous to *C. elegans* CED-4, participates in cytochrome *c*-dependent activation of caspase-3. *Cell* 90, 405–413 (1997).
14. Li, P. *et al.* Cytochrome *c* and dATP-dependent formation of Apaf-1/Caspase-9 complex initiates an apoptotic protease cascade. *Cell* 91, 479–489 (1997).
15. Srinivasula, S. M., Ahmad, M., Fernandes-Alnemri, T. & Alnemri, E. S. Autoactivation of procaspase-9 by Apaf-1-mediated oligomerization. *Mol. Cell* 1, 949–957 (1998).
16. Yang, X., Chang, H. Y. & Baltimore, D. Essential role of CED-4 oligomerization in CED-3 activation and apoptosis. *Science* 281, 1355–1357 (1998).
17. Hu, Y., Ding, L., Spencer, D. M. & Nunez, G. WD-40 repeat region regulates Apaf-1 self-association and procaspase-9 activation. *J. Biol. Chem.* 273, 33489–33494 (1998).
18. Zou, H., Li, Y., Liu, X. & Wang, X. An APAF-1-cytochrome *c* multimeric complex is a functional apoptosome that activates procaspase-9. *J. Biol. Chem.* 274, 11549–11556 (1999).
19. Saleh, A., Srinivasula, S. M., Acharya, S., Fishel, R. & Alnemri, E. S. Cytochrome *c* and dATP-mediated oligomerization of Apaf-1 is a prerequisite for procaspase-9 activation. *J. Biol. Chem.* 274, 17941–17945 (1999).
20. Du, C., Fang, M., Li, Y., Li, L. & Wang, X. Smac, a mitochondrial protein that promotes cytochrome *c*-dependent caspase activation by eliminating IAP inhibition. *Cell* 102, 33–42 (2000).
21. Verhagen, A. *et al.* Identification of DIABLO, a mammalian protein that promotes apoptosis by binding to and antagonizing inhibitor of apoptosis (IAP) proteins. *Cell* 102, 43–53 (2000).
22. Deveraux, Q. L. *et al.* Cleavage of human inhibitor of apoptosis protein XIAP results in fragments with distinct specificities for caspases. *EMBO J.* 18, 5242–5251 (1999).
23. Takahashi, R. *et al.* A single BIR domain of XIAP sufficient for inhibiting caspases. *J. Biol. Chem.* 273, 7787–7790 (1998).
24. Liu, X., Zou, H., Slaughter, C. & Wang, X. DFF, a heterodimeric protein that functions downstream of caspase-3 to trigger DNA fragmentation during apoptosis. *Cell* 89, 175–184 (1997).
25. Enari, M. *et al.* A caspase-activated DNase that degrades DNA during apoptosis, and its inhibitor ICAD. *Nature* 391, 43–50 (1998).
26. Liu, X. *et al.* The 40-kDa subunit of DNA fragmentation factor induces DNA fragmentation and chromatin condensation during apoptosis. *Proc. Natl Acad. Sci. USA* 95, 8461–8466 (1998).
27. Hirel, P.-H., Schmitter, J.-M., Dessen, P., Fayat, G. & Blanquet, S. Extent of N-terminal methionine excision from *Escherichia coli* proteins is governed by the side-chain length of the penultimate amino acid. *Proc. Natl Acad. Sci. USA* 86, 8247–8251 (1989).
28. Rotonda, J. *et al.* The three-dimensional structure of apopain/CPP32, a key mediator of apoptosis. *Nature Struct. Biol.* 3, 619–625 (1996).
29. Hauck, R. E., Munji, G. A. & Friesen, P. D. The BIR motifs mediate dominant interference and oligomerization of inhibitor of apoptosis Op-IAP. *Mol. Cell. Biol.* 20, 1877–1885 (2000).
30. Sun, C. *et al.* NMR structure and mutagenesis of the inhibitor-of-apoptosis protein XIAP. *Nature* 401, 818–822 (1999).
31. Liu, X., Kim, C. N., Yang, J., Jemmerson, R. & Wang, X. Induction of apoptotic program in cell-free extracts: Requirement for dATP and cytochrome *c*. *Cell* 86, 147–157 (1996).
32. Terwilliger, T. C. & Berendzen, J. Correlated phasing of multiple isomorphous replacement data. *Acta Crystallogr. D* 53, 749–757 (1996).
33. Collaborative Computational Project, N. The CCP4 suite: programs for protein crystallography. *Acta Crystallogr. D* 50, 760–763 (1994).
34. Jones, T. A., Zou, J.-Y., Cowan, S. W. & Kjeldgaard, M. Improved methods for building protein models in electron density maps and the location of errors in these models. *Acta Crystallogr. A* 47, 110–119 (1991).
35. Brünger, A. T. *et al.* Crystallography and NMR system: A new software suite for macromolecular structure determination. *Acta Crystallogr. D* 54, 905–921 (1998).
36. Kraulis, P. J. Molscript: a program to produce both detailed and schematic plots of protein structures. *J. Appl. Crystallogr.* 24, 946–950 (1991).
37. Nicholls, A., Sharp, K. A. & Honig, B. Protein folding and association: Insights from the interfacial and thermodynamic properties of hydrocarbons. *Proteins* 11, 281–296 (1991).

Acknowledgements

We thank D. Vaux for providing XIAP cDNA; E. Alnemri for providing caspase-3 expression vector; F. Hughson for critically reading the manuscript; and N. Hunt for secretarial assistance. This work was supported by start-up funds from Princeton University (to Y.S.) and Howard Hughes Medical Institute (to K.W.). Y.S. is a Searle Scholar and a Rita Allen Scholar.

Correspondence and requests for materials should be addressed to Y.S. (e-mail: yshi@molbio.princeton.edu). The atomic coordinates have been deposited with the Protein Data Bank with the accession number 1FEW.